Robust Leak Tests for Transmission Systems Using Nonlinear Mixed-Effect Models

KAMRAN PAYNABAR
Georgia Institute of Technology, Atlanta, GA, 30332

JIONGHUA (JUDY) JIN
University of Michigan, Ann Arbor, MI 48109

JOHN AGAPIOU
General Motors R&D, Warren, MI 48090

PAULA DEEDS
General Motor Powertrain, Pontiac, MI 48340

Problem: Leakage of the transmission fluid or oil in powertrain systems (i.e., transmissions, cylinder heads, engine blocks, etc.) can cause engine overheating and/or permanent damage. Therefore, it is crucial to run a leak test to inspect for any possible porosity in the casting parts. However, the inspection results for the amount of leakage at given testing times are sensitive to the tested part's temperature, which varies from part to part but was not previously incorporated in the leak testing systems. The objective of this paper is to develop a robust leak testing system that is insensitive to the part temperature variations in real production processes.

Approach: In the production line, a part is tested at a temperature that is generally not equal to the calibration temperature at which the inspection threshold for leakage was set. To achieve a robust leak test that is insensitive to temperature variation in the tested part, we propose a temperature compensation algorithm to adjust the measured leak flow, taking into account the tested part temperature and the calibration temperature. For this purpose, a nonlinear mixed-effect model is first developed for modeling the leak flow profile as a function of both the leak testing time and the part temperature. Then, the fitted mixed-effect model is used to adjust the leak flow based on the calibration temperature. If the amount of the adjusted leakage at the given inspection time exceeds the inspection threshold, the part is rejected; otherwise, the part is accepted.

Results: The proposed compensation algorithm is developed and validated using a set of training samples and another set of test samples, respectively. We use the percentage of error reduction in the leak flow measurements at different temperatures as the criterion to validate the developed compensation algorithm. The results show that the average percentage of error reduction for the test samples is about 92%. This indicates a significant improvement in the leak testing results.

Key Words: Control Charts; Nonlinear Profiles; Parametric Nonlinear Regression; Powertrain Manufacturing; Random Effects.

Process Description

SURFACE porosity is one of the most frequent defects in casting metal parts such as transfer cases in a transmission system. Moreover, internal porosity within a casted part could lead to surface porosity after machining. This problem is caused when gas is trapped in the metal as the casting solidifies, creating voids in the material. Although surface pores are typically smaller than 0.5 mm, they may cause significant leakage of transmission fluid and severe damage to the transmission system. The occurrence of pores (voids) on the surface of casting parts is a critical concern in powertrain manufacturing. Therefore, it is pertinent to inspect for porosity or leakage in casting parts to avoid excessive transmission fluid leakage.

One available leak testing method uses the microflow gas testing technology invented by Advance Test Concepts (ATC) Inc. (Sagi et al. (1999)). In this method, either compressed air or helium is used as the medium to measure the leak in casting parts. The amount of transitional flow from the compressed air tank to the tested part, which is measured by an intelligent gas leak sensor (IGLS), is the surrogate measure of leak flow. Details of the leak testing procedures are described as follows.

A complete leak testing procedure consists of four steps—standby, fill, stabilize, and test—as shown in Figure 1. At the standby step, the tested part, also called the unit under test (UUT), is attached to the test-bed fixture to isolate the critical cavities to be tested for open porosity. At the fill step, the part is filled with air using a compressed air tank. To reduce the test's setup time, the compressed air is mainly pushed through the lower channel, which is much wider than the upper channel, with the IGLS. It should be noted that at this fill step, the lower channel valve is open for air to pass through. The stabilize step is used for the whole testing system to achieve a stable airflow and pressure throughout the channels and the UUT. Finally, at the test step, the air tank and lower channel valves are all closed. Therefore, the high-pressure air in the channel can only pass through the upper channel if the UUT has a leak. A typical test cycle is about 40 seconds. Figure 2 shows a leak flow signal obtained during the stabilize and test steps. As can be seen from Figure 2, after the stabilize step, the leak flow measured by the IGLS has a nonlinear upward trend. At the end of the test, if the leak flow exceeds a predefined inspection threshold, the tested part is rejected as a nonconforming part due to unacceptably high leakage. The inspection threshold is denoted by U, and in this study, $U = 0.29$ cc/min is used.

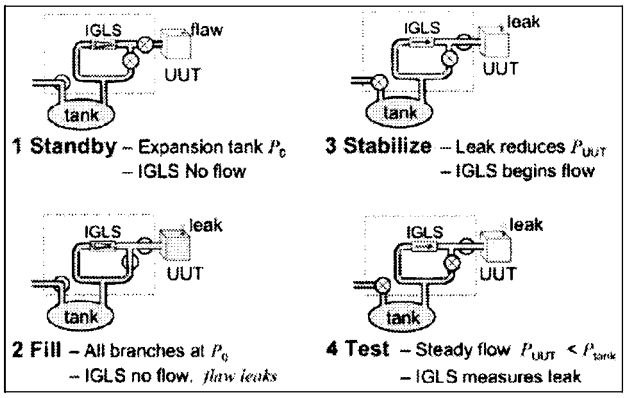

FIGURE 1. Four Steps of the Leak Test. (Courtesy of ATC Inc.)

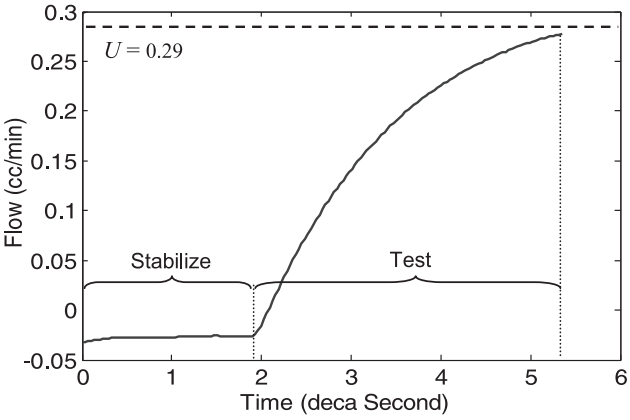

FIGURE 2. Leak Flow Profile versus Time during the Leak Test.

Dr. Paynabar is an Assistant Professor in the H. Milton Stewart School of Industrial and Systems Engineering at Georgia Tech. His email address is kamip@umich.edu.

Dr. Jin is a Professor in the Department of Industrial and Operations Engineering. Her email address is jhjin@umich.edu.

Dr. John Agapiou is a technical fellow at the General Motors Research & Development Center. His email address is John.agapiou@gm.com.

Ms. Deeds is an engineering manager at the General Motors Casting, Engine and Transmission Center. Her email address is Paula.J.Deeds@gm.com.

One critical problem in the above leak testing system is that the measured leak flow is sensitive to differences in the part temperatures among different UUTs, because the part temperature may affect the temperature of air used as the medium in the leak test or may influence the size of porosity due to thermal expansion. In practice, part temperature variation is inevitable and is caused by both environmental conditions and production processes. For example, prior to conducting leak tests, parts are often washed by passing through hot water and a dryer to remove contaminants, and the parts' temperatures are elevated after the washing process. Generally, in order to balance a production line, multiple leak testing stations are operated simultaneously, where the distances between the washing station and different testing stations are different. Therefore, after the washing operation, different parts may have different cooling times before arriving at their designated testing stations. Moreover, seasonal and daily environmental temperature differences may cause changes in the ambient temperature of production processes. In practice, controlling those factors that cause the temperature variations would be impractical or costly in powertrain production processes. Yet it is desirable that the leak testing system be standardized so that the test results of a part at different manufacturing sites are consistent. Generally, the inspection threshold for detecting unacceptably high leakages must be preset at a calibration stage by using standard "master" parts. Master parts are parts with preknown leakage status that are used to calibrate the leak testing machine by determining the proper inspection threshold. The part temperature used at this calibration stage is called the *calibration temperature*, which is equal to 72°F and denoted by T_0 in the paper. During production, each individual part's temperature may differ from this calibration temperature. As a result, when this preset inspection threshold is used for a UUT having a temperature that differs from the calibration temperature, the testing result may incorrectly classify the leakage status of the UUT.

To illustrate the effect of part temperature on the measured leak flow profile, one part was tested under two different temperatures, and the test was repeated three times at each temperature level. Figure 3 shows the corresponding six profiles of the measured leak flows. Notice that, at each temperature, two of the profiles are nearly identical. In this experiment, the elevated temperature (78°F) corresponds to the situation when the part is quickly transferred

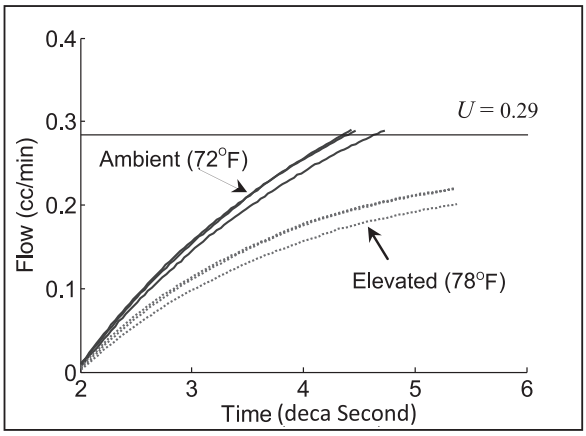

FIGURE 3. The Effect of Temperature on Leak Flow Profiles.

to the testing station right after the washing operation, while the low temperature is associated with the test condition when the part has cooled down to ambient temperature (72°F). As shown in Figure 3, when the part is tested at ambient temperature, the measured leak flow exceeds the inspection threshold, in which case the part would be rejected. In contrast, when the same part is tested at the elevated temperature, the measured leak flow is below the inspection threshold, in which case the part would not be rejected. Therefore, ignoring the effect of part temperature may result in an increase of either the false alarm rate or the missed-detection rate of the leak testing system, depending on whether the testing temperature of the UUT is below or above the calibration temperature.

The main purpose of this paper is to improve the current leak testing system by developing a robust leak testing procedure that is insensitive to differences in part temperatures. For this purpose, a statistical model is developed to compensate for the effect of the part temperature on the measured leak flow. In the following sections of the paper, we first explain the experiments and data collection procedures. Then, a nonlinear mixed-effect (NLME) model is developed to describe the leak profile as a function of the testing time and part temperature. Following this, a temperature compensation algorithm is developed based on the NLME model, which is used to adjust the leak flow measured at the part temperature to the equivalent leak flow at the calibration temperature. After that, the performance of the proposed method is evaluated. Finally, concluding remarks and recommendations are presented.

Experiments and Data Collection

As the first step, parts with different leakage levels, which are identified as low-leak, marginal-leak, and high-leak parts, are selected and tested at two temperature levels: the ambient temperature and the elevated temperature when the part is tested immediately after the washing operation. Figure 4 shows the measured leak flow profiles under the two temperature levels for the three tested parts, corresponding to the low-leak, marginal-leak, and high-leak status, respectively. Based on engineering judgment, we concluded that the part temperature will not affect the inspection decision for parts that have either severe or near-zero leakage. The reason is that if there is no porosity in a part to cause any leak, the leak flow is ideally equal to zero, and the part temperature will not affect the measured leak flow as shown in Figure 4. On the other hand, if there are large porosities in a part that cause a severe leak, the measured leak flow will be so high that it always far exceeds the inspection threshold regardless of the part temperature. Therefore, the temperature compensation algorithm is only needed when the tested parts have marginal leakage that is close to the rejected criterion. Based on preliminary analyses of leak flow profiles, we consider a part to be a potential marginal-leak part if its measured leak flow is within the interval 0.08–0.45 cc/min at the end of testing time when its temperature is within the range of 72°F to 90°F. Therefore, we limit our study only to the parts with leak flow measurements of 0.08–0.45 cc/min.

At the second step of our experimental tests, 20 marginal-leakage parts were selected. Each part was tested under multiple temperatures, and the resultant leak flow profiles were recorded. The temperature range selected for these experiments covers the whole operational range within which the part temperature varies in the leak testing station. Table 1 summarizes the test conditions. As can be seen from Table 1, all parts have been tested under the calibration ambient temperature 72°F. Among these 20 parts, 15 parts are randomly selected as the training parts whose leak flow profile data are used for training the proposed NLME model. Five other parts are used for the model validation afterwards. A larger sample size would provide more accurate and precise estimates in an NLME model. However, conducting such leak test experiments for a large number of parts is cost prohibitive because the tests interrupt the normal production line by heating up or cooling down each tested part.

Since the initial time points of different leak flow profiles vary, all profiles are registered and aligned so that each leak flow profile starts from the same time origin. Figure 5 shows the aligned leak flow profiles for Part 5, tested under four different temperatures.

Analysis and Interpretation

In the literature, there are various research studies addressing the analysis of nonlinear profile data. For instance, for product quality classification and fault diagnosis purposes, Jin and Shi (2000) and Zhou and Jin (2005) used principal component analysis (PCA), combined with supervised classification methods for DOE data and unsupervised clustering methods for regular production data, respectively. To monitor

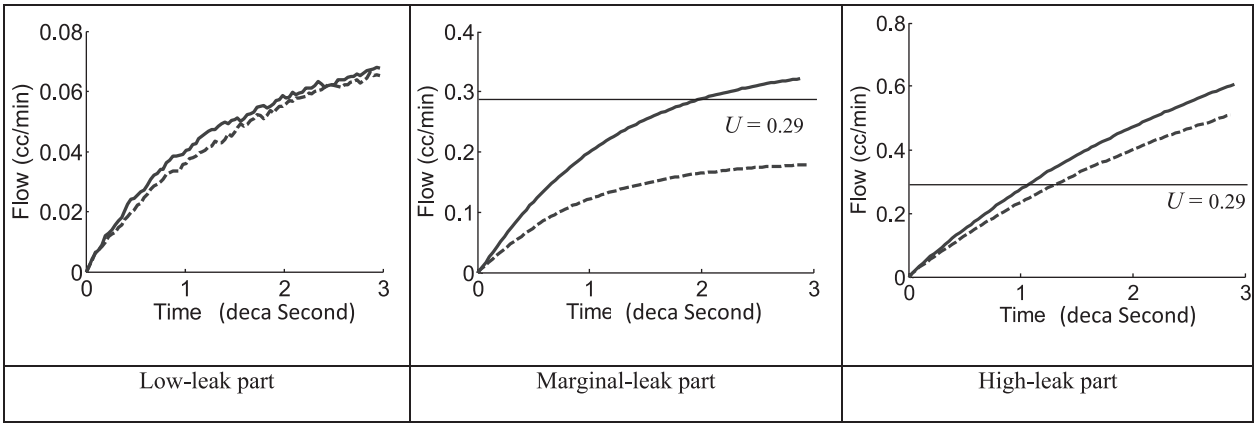

FIGURE 4. The Effect of Temperature on Leak Flow Profiles for Low-, Marginal-, and High-Leak Parts. (Solid line: ambient temperature = 72°F; dashed line: elevated temperature = 78°F.)

TABLE 1. Summary of Test Conditions for Marginal-Leak Parts

Run #	Part #	Data type	Part temperature (Fahrenheit)	Run #	Part #	Data type	Part temperature (Fahrenheit)
1	1	Training	72	36	10	Training	90
2			78	37	11	Training	72
3			80	38			74
4			83	39			76
5	2	Training	72	40			82
6			75	41	12	Training	72
7			78	42			76
8			82	43			80
9			86	44	13	Training	72
10	3	Training	72	45			82
11			78	46			84
12			82	47			89
13			83	48	14	Training	72
14			85	49			77
15	4	Training	72	50			78
16			75	51			82
17			76	52	15	Training	72
18			79	53			80
19	5	Training	72	54			84
20			75	55			90
21			78	56	16	Test	72
22	6	Training	72	57			75
23			75	58			80
24			77	59			83
25			78	60			86
26	7	Training	72	61	17	Test	72
27			78	62			76
28	8	Training	72	63			82
29			90	64	18	Test	72
30	9	Training	72	65			74
31			78	66			79
32			82	67	19	Test	72
33	10	Training	72	68			76
34			82	69	20	Test	72
35			84	70			77

nonlinear profiles, Ding et al. (2006) applied PCA and independent component analysis. Williams et al. (2007) used both parametric and nonparametric regression for nonlinear profile monitoring. Mosesova et al. (2006) and Jensen and Birch (2009) used NLME to model and monitor nonlinear profiles. Paynabar and Jin (2011) developed a wavelet-based mixed-effect model to characterize process variations for fault diagnosis. Most prior work focuses on process monitoring and diagnosis problems, in which nonlinear profiles can be represented in terms of uniform sampling of time and location. In this case study, however, the leak flow profiles not only depend on the testing time, but are affected by the temperature variable as an uncontrollable disturbance factor that can influence the inspection decision about the leakage status of a part. Moreover, the existing classification approaches in the literature cannot be effectively applied to our problem due to the continuous change of temperature levels.

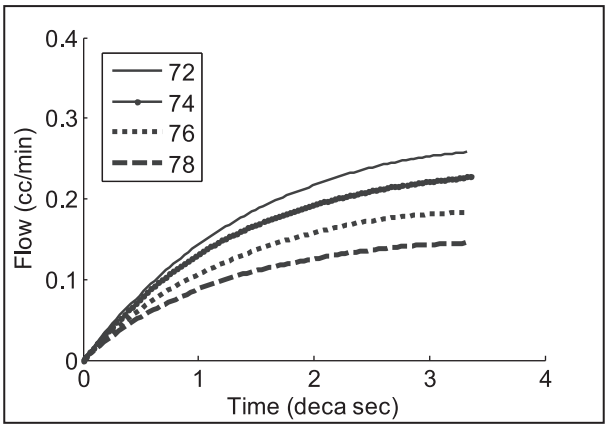

FIGURE 5. Leak Flow Profiles for Part 5 Tested under Different Temperatures.

Overview of Proposed Method

The proposed method is depicted in the flowchart in Figure 6. The methodology comprises two main phases: offline baseline training and online leak testing using the proposed temperature compensation algorithm. In the training phase, an NLME model is developed, which quantifies the leak flow of the UUT as a function of both the testing time and part temperature. As discussed previously, 15 training samples of marginal-leak parts, which were tested under multiple temperatures as shown in Table 1, are used to estimate the NLME parameters.

In the second phase of online leak testing, each incoming part after the washing station is tested, and the leak flow profile and part temperature are

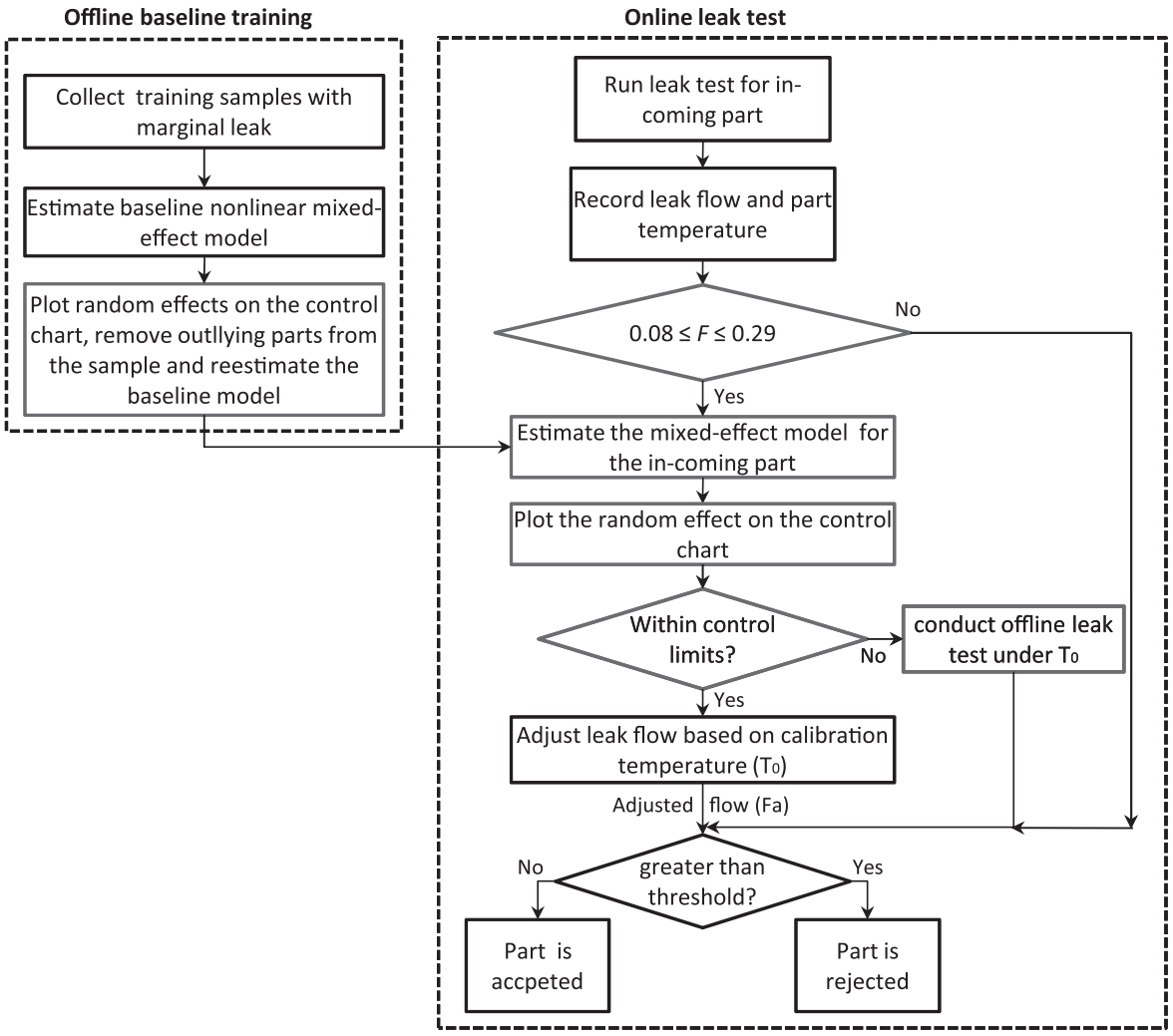

FIGURE 6. Overview of the Proposed Methodology.

recorded. Then, the recorded leak amount at the end of the testing time, denoted as F, is compared with the inspection threshold of $U = 0.29$. If F is larger than or equal to 0.29, no adjustment is needed and the part is rejected. This is because the part temperature after the washer is higher than the calibration temperature, and the leak flow increases as the part temperature decreases. Therefore, the adjusted flow is even larger than F, and the part is surely rejected. If the part is a low-leak part (i.e., $F < 0.08$) no adjustment is needed, and the part is accepted. Otherwise, the measured leak flow of the marginal part must be adjusted based on the calibration temperature before being compared with the inspection threshold.

Different parts may have different leaks, and the effect of the part's temperature on the leak flow may also depend on the level of the part's leak. Therefore, we need to estimate the leak flow function for each part in terms of both testing time and part temperature. It should be clarified that the temperature varies from part to part but is kept constant during the short testing time for each tested part. Therefore, fitting this leak flow function is quite challenging because only one temperature value exists for each part. As a result, it is impossible to estimate the temperature effect by using only one part's temperature. To overcome this issue, we identify the group of parts that have a similar leak level and are tested at different temperatures. The test data corresponding to these parts can be combined for modeling the temperature effect. As will be shown in the next section, the marginal parts collected at the training phase can be used for this purpose.

It should be noted that the training samples must be checked for potential outliers, which is done by implementing a Phase I control chart. If an outlier part is detected, it is removed from the training samples and the mixed-effect model is reestimated. This analysis is repeated until no further outlier parts are detected, and thus a baseline mixed-effect model is obtained. At the online testing stage, we pool the temperature data of the training parts and each incoming marginal part with $0.08 < F < 0.29$ to estimate the leak flow model parameters for the incoming marginal part. Then, the control chart constructed at the training phase is used to check if the incoming part's model follows the baseline model. If not, the obtained model cannot be used to perform the temperature compensation for this part, and it should be tested offline after its temperature reaches the calibration temperature. Otherwise, an estimated mixed-effect model is employed to adjust the measured leak flow profile based on the calibration temperature, henceforth called the adjusted leak flow. Finally, the adjusted leak flow at the end of testing time, denoted by F_{a}, is compared with the preset inspection threshold at the calibration temperature (i.e., $U = 0.29$). If F_{a} is less than the threshold, the part is accepted, otherwise the part is rejected. The details of the proposed method are explained in the following subsections.

Modeling Leak Flow Profiles

In order to take the effect of part temperature into account, a parametric NLME model is developed to model the measured leak flow in terms of both the testing time and part temperature. Based on engineering knowledge, the proposed model should satisfy two physical constraints. The first constraint is the initial condition, which requires all leak flow signals to start from zero. In other words, at the beginning of the testing time, the measured leak flow is set as zero across all parts and temperatures. The second condition is the limiting condition that requires the leak flow to reach a maximum stable "steady state" value if the test runs for a sufficiently long time. Additionally, as can be seen from Figure 5, the difference in the profiles at two different temperature levels becomes more pronounced at the later testing times. Therefore, the temperature effect in the model is associated with the testing time, and we include an interaction between the testing time and part temperature. Based on the shape of leak flow profiles, physical constraints, and engineering domain knowledge, we use the nonlinear model.

$$F_{ijk} = (\beta_{0i} + \beta_{1i} T_{ik})(1 - \exp\{-\beta_{2i} t_{ijk}\}) + \varepsilon_{ijk}, \quad (1)$$

where F_{ijk} is the leak flow measured for part i at time t_{ijk} with temperature T_{ik} ($i = 1, 2, \ldots, m$; $j = 1, 2, \ldots, n_i$; $k = 1, 2, \ldots, K_i$). T_{ik} is the kth temperature at which part i is tested, t_{ijk} represents the testing time for recording the jth measurements of the leak flow profile of part i tested at its kth temperature, and the ε_{ijk} are independent and identically distributed random noise variables with $\varepsilon_{ijk} \sim N(0, \sigma_{\varepsilon}^2)$.

It can be verified that the above two physical constraints are satisfied by the proposed model, i.e., that $F_{ijk} = 0$ when $t_{ijk} = 0$, and F_{ijk} attains to a steady value as $t_{ijk} \to \infty$. The exponential function structure of the proposed model is based on a first-order dynamic system model, which is often used in the

fluid dynamics literature (Franklin et al. (2006)). The model parameters can also be further interpreted as follows. $(\beta_{0i} + \beta_{1i}T_{ik})$ is the attained steady-state value of the leak flow for part i, which depends on the part temperature. β_{1i} represents the proportional effect of part temperature on the leak flow of part i, and $1/\beta_{2i}$ is the time constant of the dynamic system, which indicates how fast a dynamic system can reach its steady state.

NLME for Leak Flow Profiles

As mentioned earlier, during online leak tests, only one temperature value exists for each part (i.e., $K = 1$). Thus, it would be impossible to estimate the temperature coefficient in model (1) with only one part's temperature value. To overcome this problem, we can use the information from training marginal parts to estimate the temperature coefficient β_1 for an incoming marginal part. This can be accomplished by modeling leak flow profile data using an NLME model.

In NLME models, the effect of each variable can be modeled by fixed effects and random effects. In general, the group's profile mean is modeled by fixed effects; the profile-to-profile variations are modeled by random effects; and within-profile variations are usually captured in the model residuals. Davidian and Giltinan (1995), Pinheiro and Bates (2000), Schabenberger and Pierce (2002), and Demidenko (2004) provided comprehensive introductions to mixed-effect models. In our case, the temperature is constant within the short testing time for each part, but it varies across different testing profiles. Therefore, the nonlinear model in (1) is augmented with the random effect of the part temperature, which results in the following NLME model.

$$F_{ijk} = (\beta_{0i} + (\beta_1 + b_{1i})T_{ik})(1 - \exp\{-\beta_{2i}t_{ijk}\}) + \varepsilon_{ijk}, \quad (2)$$

where β_{0i} and β_{2i} are fixed effects for part i; β_1 is the temperature fixed effect, which is constant for all marginal parts; and b_{1i} is the temperature random effect of part i, which varies across different parts. It is assumed that b_{1i} follows a normal distribution with $b_{1i} \sim N(0, \sigma^2_{b_1})$. It should be noted that in the NLME model in (2), different β_{0i} and β_{2i} are used for each part to reflect the difference among parts. An alternative approach to model the leak flow profile is to use an NLME model with three random effects. In this case, the NLME can be written as

$$F_{ijk} = ((\beta_0 + b_{0i}) + (\beta_1 + b_{1i})T_{ik}) \times (1 - \exp\{-(\beta_2 + b_{2i})t_{ijk}\}) + \varepsilon_{ijk}, \quad (3)$$

where $\boldsymbol{\beta}^{\mathrm{T}} = [\beta_0, \beta_1, \beta_2]$ is the vector of fixed effects, which is constant across all profiles, and $\mathbf{b}_i^{\mathrm{T}} = [b_{0i}, b_{1i}, b_{2i}]$ is the vector of random effects for part i. The superscript T denotes the transpose operator. It is assumed that $\mathbf{b}_i$ follows a multivariate normal distribution, i.e., $\mathbf{b}_i \sim \mathrm{MVN}(\mathbf{0}, \boldsymbol{\Lambda})$, where $\mathbf{0}$ indicates the zero mean vector and $\boldsymbol{\Lambda}$ is the 3 by 3 covariance matrix that models part-to-part variations, and consists of the variances of random effects and their pair-wise covariances. Generally speaking, this model assumes that all leak flow profiles share the same mean, and the deviation of each profile from the mean profile, caused by part-to-part variations, can be modeled by random effects $\mathbf{b}_i$. It should be noted that the NLMEs in (2) and (3) are not nested models because the NLME model in (2) has β_{0i} and β_{2i} modeled as separate fixed effects for each part and not as random effects as in model (3).

To estimate the parameters of NLME models, both maximum likelihood and restricted maximum likelihood estimation methods can be employed (Demidenko (2004)). For this purpose, consider the matrix representation

$$\mathbf{F}_i = g(\mathbf{T}_i, \mathbf{t}_i, \boldsymbol{\beta}, \mathbf{b}_i) + \boldsymbol{\varepsilon}_i \quad (4)$$

of model (3), where $\mathbf{F}_i = [\mathbf{F}_{i1}^{\mathrm{T}}, \mathbf{F}_{i2}^{\mathrm{T}}, \ldots, \mathbf{F}_{iK_i}^{\mathrm{T}}]^{\mathrm{T}}$ with $\mathbf{F}_{ik}$ denoting the vector of measured leak flows of part i tested at temperature k, $\mathbf{T}_i = [\mathbf{T}_{i1}^{\mathrm{T}}, \mathbf{T}_{i2}^{\mathrm{T}}, \ldots, \mathbf{T}_{iK_i}^{\mathrm{T}}]^{\mathrm{T}}$ with $\mathbf{T}_{ik} = T_{ik}\mathbf{1}_{n_i}$, where $\mathbf{1}_{n_i}$ is the length-n_i vector of ones, $\mathbf{t}_i = [\mathbf{t}_{i1}^{\mathrm{T}}, \mathbf{t}_{i2}^{\mathrm{T}}, \ldots, \mathbf{t}_{iK_i}^{\mathrm{T}}]^{\mathrm{T}}$ with $\mathbf{t}_{ik} = [t_{ijk}]$ is the vector of testing times, $g(\mathbf{T}_i, \mathbf{t}_i, \boldsymbol{\beta}, \mathbf{b}_i)$ is the nonlinear function $((\beta_0 + b_{0i}) + (\beta_1 + b_{1i})\mathbf{T}_i)(1 - \exp\{-(\beta_2 + b_{2i})\mathbf{t}_i\})$, and $\boldsymbol{\varepsilon}_i = [\boldsymbol{\varepsilon}_{i1}^{\mathrm{T}}, \boldsymbol{\varepsilon}_{i2}^{\mathrm{T}}, \ldots, \boldsymbol{\varepsilon}_{iK_i}^{\mathrm{T}}]^{\mathrm{T}}$ with $\boldsymbol{\varepsilon}_{ik}^{\mathrm{T}}$ is the vector of random noise variables corresponding to the leak flow profiles of part i tested at temperature k.

The marginal distribution of $\mathbf{F}_i$ cannot be obtained in closed form, and, consequently, numerical methods are needed to obtain the MLE's. We used the Lindstrom and Bates method (Pinheiro and Bates (2000)) in this paper.

In addition to the above two NLME models, model (2) with only one random effect for β_1 and model (3) with all three random effect coefficients, there are two other possible models to be considered, i.e., one model with two random effects for β_0 and β_1, and the other with two random effects for β_2 and β_1. Therefore, we consider the four model candidates shown in Table 2. In order to estimate model coefficients for an incoming part with only one temperature value,

TABLE 2. Comparison of Nonlinear Mixed-Effect Models in Terms of Log-Likelihood and AIC

Model	Fixed effects	Random effects	Log-likelihood	AIC
1. $F_{ijk} = (\beta_{0i} + (\beta_1 + b_{1i})T_{ik}(1 - \exp\{-\beta_{2i}t_{ijk}\}) + \varepsilon_{ijk}$	β_{0i}, β_{2i}, β_1	b_{1i}	20027.76	−39993.52
2. $F_{ijk} = ((\beta_0 + b_{0i}) + (\beta_1 + b_{1i})T_{ik}) \times (1 - \exp\{-(\beta_2 + b_{2i})t_{ijk}\}) + \varepsilon_{ijk}$	β_0, β_1, β_2	b_{0i}, b_{1i}, b_{2i}	19938.96	−39857.92
3. $F_{ijk} = (\beta_{0i} + (\beta_1 + b_{1i})T_{ik}) \times (1 - \exp\{-(\beta_2 + b_{2i})t_{ijk}\}) + \varepsilon_{ijk}$	β_{0i}, β_1, β_2	b_{1i}, b_{2i}	19970.70	−39901.39
4. $F_{ijk} = ((\beta_0 + b_{0i}) + (\beta_1 + b_{1i})T_{ik}) \times (1 - \exp\{-\beta_{2i}t_{ijk}\}) + \varepsilon_{ijk}$	β_0, β_1, β_{2i}	b_{0i}, b_{1i}	19990.04	−39940.08

the temperature coefficient (β_1) must be defined as a random effect in all candidate models.

To compare the fitness performance of these four models, all models are estimated using the training data. Then, the Akaike information criterion (AIC) is calculated for each model using $\text{AIC} = 2k - 2\log(L)$, where k is the number of estimated parameters in the model, and L denotes the likelihood function value for the model (Akaike (1974)). A smaller value of AIC indicates a better fitting of the model. Table 2 shows the log-likelihood and AIC values corresponding to each model. As can be seen from Table 2, the first model has the largest log-likelihood and the smallest AIC, implying it fits our training samples the best.

Detecting Outlier Profiles in the Training Sample

Although only marginal parts are considered in the offline training phase, it is possible that one or more parts have Outlier profiles. Such Outlier profiles can affect the model training and estimation, and thus should be detected and removed from the training samples. To detect the outlier profiles, similar to Jensen and Birch (2009), we construct a control chart for monitoring random effects. Since there is only one random effect in the model, a Shewhart individuals control chart on the standardized statistic is used. The monitoring statistic denoted by Z_i, along with the lower control limit (LCL) and upper control limit (UCL), are given as

$$Z_i = \frac{b_{1i}}{S_b}; \quad \text{and} \quad \text{UCL} = -\text{LCL} = Z_{\alpha^*/2}, \qquad (5)$$

where,

$$S_b = \sqrt{\textstyle\sum_{i=1}^{m-1}(b_{1(i+1)} - b_{1i})^2/(2m-2)}$$

is an estimate of the random effects variance based on successive difference of random effects (Holmes and Mergen (1993)), $Z_{\alpha^*/2}$ is the $100(1-\alpha^*/2)$ percentile of the standard normal distribution with $\alpha^* = 1 - (1-\alpha)^{1/m}$, and α is the desired Type-I error rate of the control chart. Note that the mean of the b_{1i}'s is zero.

The statistic Z_i is plotted for each part on the control chart, and if it is beyond the control limits, it is considered as an outlier and its corresponding part is removed from the training samples. For our training samples, S_b obtained from the NLME model in (2) is 0.0678. Figure 7 shows the control chart for Z_i with control limits $\text{UCL} = -\text{LCL} = 2.9278$ corresponding to overall Type-I error rate $\alpha = 0.05$. In this case, the Type-I error rate for each comparison (sample) approximately is $1 - (1 - 0.05)^{1/15} = 0.0034$.

As can be seen in Figure 7, the random effect of Part 12 exceeds the control limits. Therefore, Part

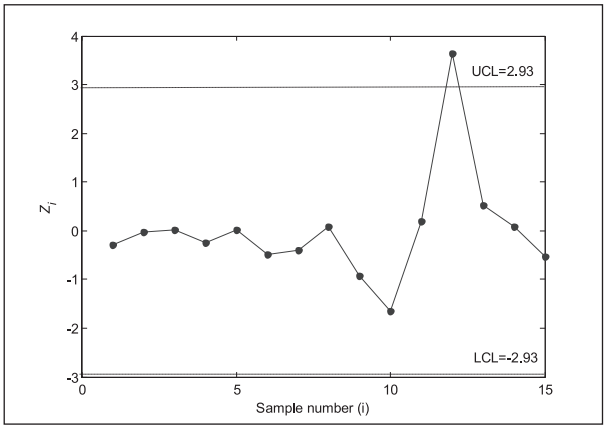

FIGURE 7. Control Chart for Estimated Random Effects.

TABLE 3. Estimated Fixed and Random Effects for Training Parts

	Fixed effects		Random effects
Part #	$\hat{\beta}_{0i}$	$\hat{\beta}_{2i}$	$\hat{b}_{1i}$
1	1.4647	0.3292	−0.0026
2	1.1442	0.8819	0.0160
3	1.0904	0.7271	0.0189
4	1.3117	0.4367	0.0016
5	1.2181	0.5432	0.0188
6	1.3036	0.7159	−0.0159
7	1.3742	0.4456	−0.0094
8	1.0284	0.3837	0.0233
9	1.8272	0.4477	−0.0445
10	2.5514	0.2855	−0.0945
11	1.0141	0.6752	0.0306
13	1.7972	0.3291	−0.0191
14	0.8161	0.8875	0.0528
15	1.2104	0.4340	0.0240

12 is removed from the training samples and the NLME model is retrained. Repeating this procedure, the control chart is reconstructed based on the new estimated random effects obtained from the retrained model. As no new outlier is detected, the estimated NLME model can be used as the baseline model. Table 3 gives the estimated fixed and random effects of the retrained NLME model after removing Part 12. The estimated fixed effect for temperature is $\hat{\beta}_1 = -0.1261$, and the estimated variance parameters are $\hat{\sigma}^2_{b_1} = 0.0013$ and $\hat{\sigma}^2_{\varepsilon} = 2.22\text{e}^{-5}$.

Figure 8 shows the measured leak flow profiles and their corresponding overlaid fits for four parts obtained from the final NLME model. As shown in this figure, the leak flow profiles can be well modeled by the proposed NLME in (2).

Online Leak Tests

As shown in the overview diagram in Figure 6, when an incoming part is tested, if the leak flow is

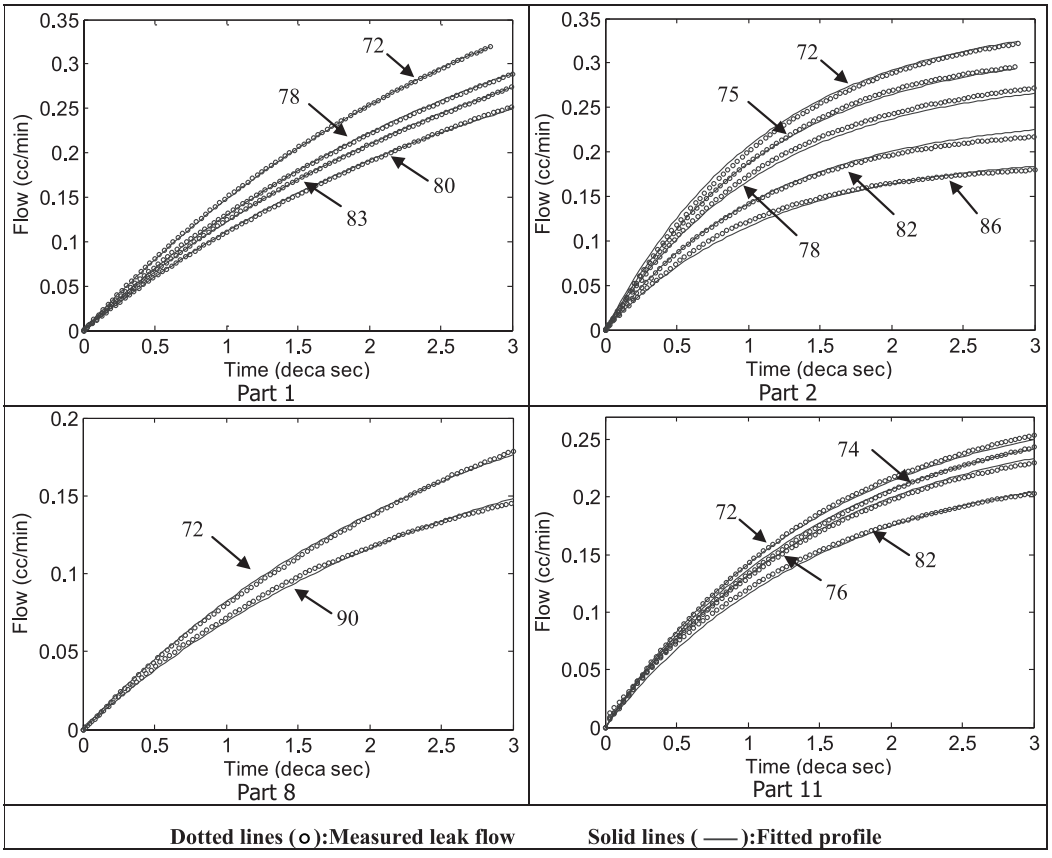

FIGURE 8. Measured Leak Flow and Fitted Profiles Obtained from the NLME Model. (Dotted lines: measured leak flow; solid lines: fitted profile.)

higher than 0.29, no adjustment is needed for the leak flow profile, and the part is rejected. If the part is a low-leak part, no adjustment is needed, and the part is accepted. Otherwise, the part is marginal-leak, and its measured leak flow must be adjusted based on the calibration temperature before being compared with the inspection threshold. For this purpose, the NLME is estimated based on the leak flow profile of the incoming part and the baseline training model. This model is employed to adjust the measured leak flow profile at the calibration temperature. Let $\hat{\boldsymbol{\beta}}_{\text{new}} = [\hat{\beta}_{0\text{new}}, \hat{\beta}_{1\text{new}}, \hat{\beta}_{2\text{new}}]^{\text{T}}$ denote the estimated vector of fixed effects for the new part and $\hat{b}_{1\text{new}}$ denote the estimated random effect for the incoming part. The next step is to check whether the incoming part follows the same model as the estimated model for the training parts. This is done by comparing $Z_{\text{new}} = b_{1\text{new}}/S_b$ with $\text{UCL} = -\text{LCL} = Z_\alpha$. If Z_{new} is beyond the control limits, it implies that this is an outlier profile; and thus the adjustment algorithm will not be valid for this part. In this situation, the leak test for this part must be conducted offline after the part cools down to the calibration temperature. If Z_{new} is within the control limits, the estimated mixed model is used to adjust the leak flow. The adjusted leak flow profile based on the calibration temperature is

$$\hat{F}_{\text{a}|T_0,t} = (\hat{\beta}_{0\text{new}} + (\hat{\beta}_{1\text{new}} + \hat{b}_{1\text{new}})T_0) \times (1 - \exp\{-\hat{\beta}_{2\text{new}}t\}), \quad (6)$$

where $\hat{F}_{\text{a}|T_0,t}$ is the adjusted leak flow profile at the given calibration temperature T_0. At the last step of the flowchart in Figure 6, the adjusted leak flow at the end of testing time t_e (denoted by $\hat{F}_{\text{a}|T_0,t_e}$) is compared with the inspection threshold U. The part is accepted if $\hat{F}_{\text{a}|T_0,t_e}$ does not exceed the threshold, i.e., if $\hat{F}_{\text{a}|T_0,t_e} \le U$, where $t_e = 3$ deca Second is used in our case study.

Performance Evaluation of the Proposed Method

To evaluate the performance of the proposed method, in addition to the training parts, we use five test parts whose leak flow profile data were not used in constructing the NLME model at the training stage. For each marginal part, the measured leak flows under the actual part temperatures are adjusted to the equivalent leak amount at the calibration temperature, using the proposed NLME model. Then the adjusted leak flow is compared to the actual leak flow measured at the calibration temperature. The criterion used for the performance evaluation is the percentage of error reduction ($\Delta\%$) after applying the proposed temperature compensation algorithm, which is calculated as:

$$\Delta\% = \left(1 - \frac{\left|F_{m|T_0,t_e} - \hat{F}_{\text{a}|T_0,t_e}\right|}{\left|F_{m|T_0,t_e} - F_{m|T_p,t_e}\right|}\right) \times 100, \quad (7)$$

where, $F_{m|T_0,t_e}$ and $F_{m|T_p,t_e}$ are the measured leak flow at the end of testing time t_e under the calibration temperature T_0 and the actual part temperature T_p, respectively. As shown in Figure 9, the denominator in Equation (7), i.e., the absolute difference of $F_{m|T_0,t_e}$ and $F_{m|T_p,t_e}$, represents the amount of original measurement errors without employing the temperature compensation. The numerator in Equation (7), i.e., the absolute difference of $F_{m|T_0,t_e}$

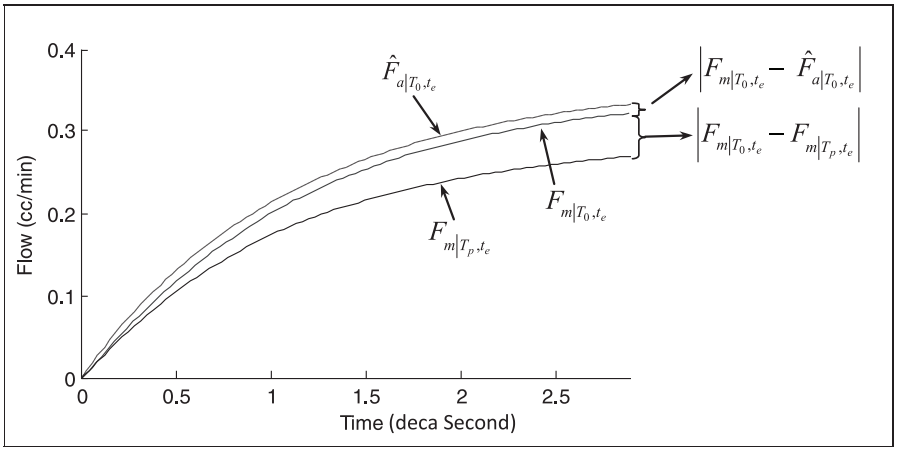

FIGURE 9. Profiles of Adjusted and Measured Leak Flow at Calibration Temperature, and Measured Leak Flow at Part Temperature.

TABLE 4. Performance Evaluation Results for Training and Test Datasets

Run #	Part #	Data type	Part temperature (Fahrenheit)	Δ%	Average Δ%	Run #	Part #	Data type	Part temperature (Fahrenheit)	Δ%	Average Δ%
1	1	Training	72	N/A	99.48%	37	11	Training	72	N/A	80.51%
2			78	99.30%		38			74	68.24%	
3			80	99.50%		39			76	81.11%	
4			83	99.65%		40			82	92.19%	
5	2	Training	72	N/A	95.34%	44	13	Training	72	N/A	91.12%
6			75	90.48%		45			82	87.54%	
7			78	95.46%		46			84	91.16%	
8			82	97.32%		47			89	94.65%	
9			86	98.10%		48	14	Training	72	N/A	82.87%
10	3	Training	72	N/A	94.09%	49			77	71.50%	
11			78	88.36%		50			78	83.36%	
12			82	95.32%		51			82	93.76%	
13			83	95.93%		52	15	Training	72	N/A	85.52%
14			85	96.77%		53			80	77.21%	
15	4	Training	72	N/A	91.47%	54			84	87.13%	
16			75	89.47%		55			90	92.22%	
17			76	91.07%		56	16	Test	72	N/A	94.94%
18			79	93.86%		57			75	92.63%	
19	5	Training	72	N/A	83.42%	58			80	94.85%	
20			75	80.20%		59			83	95.52%	
21			78	86.63%		60			86	96.78%	
22	6	Training	72	N/A	95.27%	61	17	Test	72	N/A	97.46%
23			75	93.35%		62			76	96.59%	
24			77	95.90%		63			82	98.33%	
25			78	96.56%		64	18	Test	72	N/A	82.20%
26	7	Training	72	N/A	92.45%	65			74	70.26%	
27			78	92.45%		66			79	94.15%	
28	8	Training	72	N/A	88.66%	67	19	Test	72	N/A	87.09%
29			90	88.66%		68			76	87.09%	
30	9	Training	72	N/A	86.74%	69	20	Test	72	N/A	94.34%
31			78	85.46%		70			77	94.34%	
32			82	88.02%							
33	10	Training	72	N/A	82.25%						
34			82	70.78%							
35			84	82.93%							
36			90	93.05%							

and $\hat{F}_{\mathrm{a}|T_0,t_e}$, represents the amount of remaining errors after employing the temperature compensation. Therefore, the fraction

$$\frac{\left|F_{m|T_0,t_e} - \hat{F}_{\mathrm{a}|T_0,t_e}\right|}{\left|F_{m|T_0,t_e} - F_{m|T_p,t_e}\right|}$$

represents the ratio of the remaining error after employing temperature compensation to the original error without temperature compensation. Equivalently, Δ% shows the percentage of the measurement error reduction after employing the proposed method. Δ% is always between 0% and 100%, Δ% = 100% indicates the perfect compensation performance.

In order to calculate Δ% for the training parts, the NLME baseline model is used to estimate the ad-

justed leak flow ($\hat{F}_{a|T_0,t_e}$). For a test part, its NLME model is estimated based on all in-control leak flow profile data from the training parts and the incoming test part. It should be mentioned that the estimated random effects for all test parts were in-control, which implies that the estimates for adjusted leak flow for the test parts are valid.

The detailed validation results are reported in Table 4. For each part, the index $\Delta\%$ is calculated under different part temperatures. The average $\Delta\%$ for each part is also given in this table. For example, for the training Part 6, if the part temperature is 77, $\Delta\%$ is 95.90%, and the average $\Delta\%$ of Part 6 under all tested temperatures is 95.27%. As can be seen from the values of $\Delta\%$ in Table 4, the performance of the adjustment algorithm improves as temperature increases. The reason is that, as expected, the adjusted flows obtained from the fitted NLME model for all temperatures are similar, which result in similar amounts of remaining errors ($|F_{m|T_0,t_e} - \hat{F}_{a|T_0,t_e}|$) after employing the temperature compensation. On the other hand, as temperature increases, the amount of error ($|F_{m|T_0,t_e} - F_{m|T_p,t_e}|$) in the flow leak caused by temperature increases. Therefore $\Delta\%$ increases as temperature increases. In short, the high values of $\Delta\%$ imply high accuracy of the proposed approach. The overall average $\Delta\%$ for all in-control training parts and the test parts are 89.60% and 92.05%, respectively. This indicates that our proposed model performs very well for both the training parts and the test parts.

Conclusions

In this study, we addressed a critical issue in the existing leak testing system (which uses air to fill cavities) for inspecting for leaks in casting parts. Our study showed that the leak testing system is sensitive to the part temperature, which may lead to incorrect quality inspection results for the marginal-leak parts. To deal with this problem, we developed a temperature compensation algorithm using the NLME model that can adjust the actual leak flow profiles measured at the actual part temperature to the equivalent leak flow at a specified calibration temperature. In this way, the adjusted leak flow can be directly compared with the quality inspection threshold that is preset at the calibration temperature. The proposed temperature compensation algorithm was validated using both training and test parts. The results showed that the algorithm can improve the performance of the current leak testing system by reducing measurement errors by 92%, on average. Utilizing such a compensation algorithm, the improved leak testing system can provide consistent leak testing decisions at different stations or plants regardless of how part temperatures vary due to inevitable variation in environmental or production conditions.

Acknowledgments

The research is jointly supported by the NSF Grant: DMI F0541750; Engineering Research Center for Reconfigurable Manufacturing Systems (NSF Grant EEC-9529125) at the University of Michigan; and General Motors Corporation. The authors would like to thank Amir Sadrpour, Sorour Talebi, Qiang Li, and Prasanna Srinivasan for their help on the experimental tests and data collection. Special thanks also go to Sunil Nandwani, Paul Tanis, and Amir Sadrpour for helping us understand the process and prepare and conduct the tests. The authors also thank the Editor and Referees for their insightful comments.

References

Akaike, H. (1974). "A New Look at the Statistical Model Identification". *IEEE Transactions on Automatic Control* 19, pp. 716–723.

Davidian, M. and Giltinan, D. M. (1995). *Nonlinear Models for Repeated Measurements Data*. London, UK: Chapman and Hall.

Demidenko, E. (2004). *Mixed Models: Theory and Applications*. New York, NY: Wiley.

Ding, Y.; Zeng, L.; and Zhou S. (2006). "Phase I Analysis for Monitoring Nonlinear Profiles in Manufacturing Processes". *Journal of Quality Technology* 38, pp. 199–216.

Franklin, G. F.; Powell, J. D.; and Emami-Naeini, A. (2006). *Feedback Control of Dynamic Systems*. Upper Saddle River, NJ: Prentice Hall.

Holmes, D. S. and Mergen, A. E. (1993). "Improving the Performance of the T2 Control Chart". *Quality Engineering* 5, pp. 619–625.

Jensen, W. A. and Birch, J. B. (2009). "Profile Monitoring via Nonlinear Mixed Models". *Journal of Quality Technology* 41, pp. 18–34.

Jin, J. and Shi, J. (2000). "Diagnostic Feature Extraction from Stamping Tonnage Signals Based on Design of Experiments". *ASME Transactions, Journal of Manufacturing Science and Engineering* 122, pp. 360–369.

Mosesova, S. A.; Chipman, H. A.; MacKay, R. J.; and Steiner, S. H. (2006). "Profile Monitoring Using Mixed-Effects Models". Technical Report RR-06-06, University of Waterloo.

Paynabar, K. and Jin, J. (2011). "Characterization of Nonlinear Profiles Variations Using Mixed-Effect Models and Wavelets". *IIE Transactions on Quality and Reliability* 43, pp. 275–290.

Pinheiro, J. C. and Bates, D. M. (2000). *Mixed-Effects Models in S and S-PLUS*. New York, NY: Springer-Verlag.

Sagi, N. H.; Zhang, G. R.; and Ghosh, R. R. (1999). Intelligent Gas Flow Measurement and Leak Detection Apparatus. U.S. Patent, Patent No. 5,861,546.

Schabenberger, O. and Pierce, F. J. (2002). *Contemporary Statistical Models for the Plant and Soil Sciences*. Boca Raton, FL: CRC Press.

Williams, J. D.; Woodall, W. H.; and Birch, J. B. (2007). "Statistical Monitoring Of Nonlinear Product and Process Quality Profiles". *Quality & Reliability Engineering International* 23, pp. 925–941.

Zhou, S. and Jin, J. (2005). "Automatic Feature Selection for Unsupervised Clustering of Cycle-based Signals in Manufacturing Processes". *IIE Transactions on Quality and Reliability* 37, pp. 569–584.